Proceedings of IMECE'03
2003 ASME International Mechanical Engineering Congress
Washington, D.C., November 15–21, 2003

IMECE2003-42682

DESIGN AND FABRICATION OF A HIGH EFFICIENCY PIEZOELECTRIC VIBRATION-INDUCED MICRO POWER GENERATOR

Gou-Jen Wang
Department of Mechanical Engineering
National Chung-Hsing University, Taiwan

Ying-Hsu Lin
Department of Mechanical Engineering
National Chung-Hsing University, Taiwan

His-Harng Yang
Institute of Precision Engineering
National Chung-Hsing University, Taiwan

Cheng-Tang Pan
Mechanical Industry Research Laboratories
Industrial Technology Research Institute, Taiwan

ABSTRACT

To fulfill the increasing self-power demanding of the embedded and remote microsystems, theoretical and experimental study of a piezoelectric vibration-induced micro power generator that can convert mechanical vibration energy into electrical energy is presented. A complete energy conversion model regarding the piezoelectric transducer is discussed first. To verify the theoretical analysis, two clusters of transducer structures are fabricated. The piezoelectric lead zirconate titanate (PZT) material that has better energy conversion efficiency among the piezoelectric materials is chosen to make of the energy conversion transducer. The desired shape of the piezoelectric generator with its resonance frequency in accordance with the ambient vibration source is designed by finite element analysis (FEA) approach.

Conducting wires and load resistor are soldered on the electrodes to output and measure the vibration induced electrical power. Experimental results shows that the maximum output voltages are generated at the first mode resonance frequencies of the structure. It is also found from the experimental results that the induced voltage is irrelevant to the width of the structure but is inverse proportion to the length of the structure. It takes 7 minutes to charge a 10,000 μF capacitors array to a 7 V level. The total amount of electricity and energy stored in the capacitors are 0.7 Coulomb and 0.245 J, respectively. The experimental results are coincidence with the theoretical analysis.

INTRODUCTION

Most of the highlights in MEMS have been on microsensors and microactuators. In many applications, embedded and remote systems are getting more attraction. The problem encountered is that the microsystems need to have their own power supply. One of the possible solutions is to design the power supply at the same scale as sensors, actuators, and electronics. Batteries are the commonly used devices. Due to disadvantages such as limited amount of energy, relatively short life duration, and possibly chemical contaminations, batteries are not so desirable. An imperative alternative to battery is embedded power supplies which provide renewable power.

Usually, a power supply has four main components: (1) a source of energy (2) a device to convert energy (3) an energy storage device (4) a mechanism to provide actuation [1]. Energy from the ambient is the idealist energy sources for a micro scale power supply. Possibly ambient energy sources includes: (1) thermal energy [2] (2) light energy (3) volume flow (4) mechanical energy. In many applications, for example, sensors and actuators in an implanted biomedical device, access to the light, thermal, or flow is greatly reduced. Mechanical energy is a more feasible ambient energy source.

A mechanical energy based power supply is designed to convert mechanical vibration into electrical energy. Three electromechanical devices can be implemented to convert the energy; (1) piezoelectric: using piezoelectric material to generate electrical potential [3-5] (2) electromagnetic [6-11]: coil attached to a mass which vibrates through a magnetic field to induce voltage according to Faraday's law (3) electrostatic:

inducing a capacitor voltage through the movements of a mass which has its permanent charges electrically arranged. Among these three mechanisms, the electrostatic transducer has lower converting efficiency; therefore, its application is limited. The electromagnetic mechanism that operates under the more familiar principle attracts the researchers the most. However, it includes a magnetic component and a coil, which in turn makes the fabrication more complicate. According to the Faraday's low, larger induced voltage requires larger amount of magnetic flux or fast vibration. The former will enlarge the volume of the device while fast vibration always is not controllable. The real applications of the electromagnetic transducer need further investigation. On 2001, Glynne-Jones et al. [3] used a simple mechanical-electrical analogous model to investigate the feasibility of a piezoelectric micro power generator. Following, Kang et al. [4] used a microbubble generator to realize the power generation. Kasyap et al., [5] then proposed a more complete model that used a transformer to represent the energy conversion mechanism. However, this linear transformer representation seems not enough to fully describe the mechanical-electrical energy mechanism, especially when an external load resistance is applied.

In this article, the modeling and fabrication of a piezoelectric based power generator is presented. In stead of the linear transform, the mechanical-electrical energy conversion mechanism is represented by a voltage controlled voltage sources between two capacitors which belongs to the mechanical and the piezoelectric equivalent circuits, respectively. To verify the theoretical analysis, two clusters of micro transducers are designed and fabricated. The desired shape of the piezoelectric generator with its resonance frequency in accordance with the ambient vibration source is designed by finite element analysis (FEA) approach. The sintering method is implemented to fabricate the piezoelectric lead zirconate titanate (PZT) film. The PZT film with 1 μm thickness of silver electrode layer being screen printed on both sides is adhered onto the top surface of the copper substrate. A micro CNC is used to cut the copper substrate into the desired shape.

PRINCIPLE OF THE PIEZOELECTRIC VIBRATION-INDUCED POWER GENERATOR

Vibration-Induced Power Generating Principle

A vibration-induced power generator is a device that functions to convert mechanical vibration into electrical energy. Figure 1 depicts the schematic model of a simple vibration-induced power generator.

Where,

m: the mass of the beam

k: the equivalent spring constant

y(*t*): the absolute displacement applied to the rigid housing and is the input to the system

x(*t*): the absolute displacement of the mass and is the output of the system

z(*t*) = *x*(*t*)-*y*(*t*): relative velocity of the mass

b: damping coefficient that includes the unwanted energy loss and the real extracted power from the system

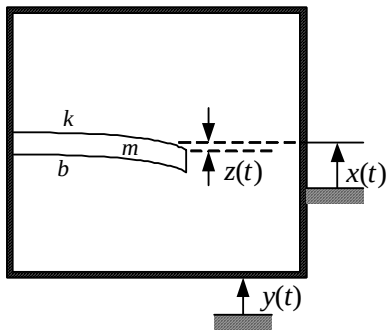

Figure 1. Schematic model of the vibration-induced power generator

The system can be modeled as

$$m\ddot{x}(t) + d\left[\dot{x}(t) - \dot{y}(t)\right] + k\left[x(t) - y(t)\right] = 0 \quad (1)$$

or

$$m\ddot{z}(t) + d\dot{z}(t) + kz(t) = -m\ddot{y}(t) \quad (2)$$

Taking Laplace transformation on the above equation, it becomes

$$-ms^2Y(s) = sZ(s)\left[ms + \frac{k}{s} + b\right] \quad (3)$$

The Thevenin equivalent circuit is

$$-V_{in}(s) = I(s)[Ls + \frac{1}{Cs} + R] \quad (4)$$

$V_{in}(s)$ denotes the voltage source and is analogous to the input force. $I(s)$ is the loop current and is analogous to the relative velocity of the mass. The analogy between Equation (3) and Equation (4) are

$$V_{in}(s) = ms^2Y(s)\ ,\ I(s) = sZ(s)\ ,\ C = 1/k\ ,\ R = b,$$
$$L = m \quad (5)$$

Equation (4) can be rewritten as

$$\begin{aligned} -V_{in}(s) &= \frac{1}{C}\frac{I(s)}{s} + I(s)[sL + R] \\ &= \frac{1}{C}Q(s) + I(s)[sL + R] \\ &= V_c(s) + I(s)[sL + R] \end{aligned} \quad (6)$$

The mechanical/electrical analogous of any vibrating mass can be described by Equation (6). The equivalent circuit of Equation (6) is depicted in Figure 2.

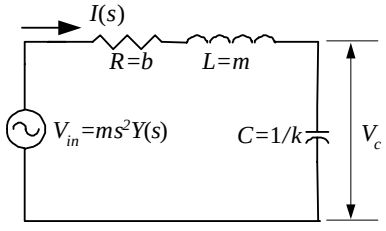

Figure 2. Equivalent circuit of the simple cantilever beam system

Principle of The Piezoelectric Power Generator

When a thin PZT film is attached to the beams as shown in Figure 3, the beam deformation will induce a potential difference V_x between the top and bottom surfaces of the PZT.

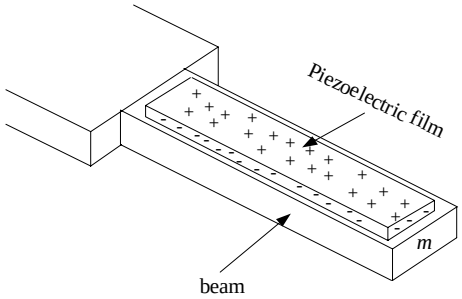

Figure 3. Schematic structure of the piezoelectric vibration-induced power generator

The PZT thin film acts as a transducer to convert the mechanical energy stored in the spring into electrical energy; therefore, the simple cantilever beam system becomes a vibration-induced power generator. The complete equivalent circuit of the vibration-induced power generator is shown in Figure 4. C_p and R_g >>0 are the equivalent capacitance and the dielectric loss of the PZT film, respectively. The induced voltage V_x on PZT can be regarded as the results of the C_p being charged by V_c.

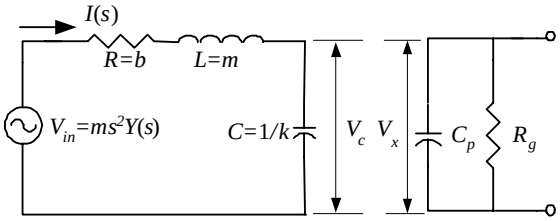

Figure 4. Equivalent circuit of the vibration-induced power generator

Assume the energy conversion rate between the mechanical energy and the electrical energy be related by the transducer electromechanical constant k_e, such that

$$k_e = \frac{1}{2}C_p V_x^2 \Big/ \frac{1}{2}CV_c^2 \tag{7}$$

The maximum instant power induced by the PZT can be described by

$$\begin{aligned} P_c(s) &= \frac{1}{2}C_p V_x^2 = \frac{1}{2}k_e C V_c^2 = \frac{1}{2}k_e C\left(\frac{I(s)}{Cs}\right)^2 \\ &= \frac{1}{2}k_e \frac{m^2 Y^2(s)s^6}{\left[ms^2+bs+k\right]^2 Cs^2} \\ &= \frac{1}{2}k_e k \frac{m^2 Y^2(s)s^4}{\left[ms^2+bs+k\right]^2} \end{aligned} \tag{8}$$

When a sinusoidal signal $y(t) = Y_0\cos(\omega t)$ is applied, Equation (8) can be rewritten as

$$\begin{aligned} \left|P_c(\omega)\right| &= \frac{kk_e m^2 Y^2(\omega)}{2}\frac{\omega^4}{\left[k-m\omega^2\right]^2+\left[\omega b\right]^2} \\ &= \frac{k_e m^2 Y^2(\omega)}{2k}\frac{\omega^4}{\left[1-\frac{m}{k}\omega^2\right]^2+\left[\frac{b}{k}\omega\right]^2} \\ &= \frac{k_e m^2 Y^2(\omega)}{2k}\frac{\omega^4}{\left[1-\left(\frac{\omega}{\omega_n}\right)^2\right]^2+\left[\frac{2\varsigma}{m}\frac{\omega}{\omega_n}\right]^2} \end{aligned} \tag{9}$$

Where,

$$\begin{aligned} \omega_n &= \sqrt{k/m} = \sqrt{1/LC} = \frac{d}{2l^2}\sqrt{\frac{E}{\rho}} \quad \text{(Appendix A)} \\ \varsigma &= \frac{b}{2\omega_n} = \frac{b}{2}\sqrt{\frac{m}{k}} = \frac{R}{2}\sqrt{LC} \end{aligned} \tag{10}$$

The ω_n in Equation (10) indicates that it is only depending on the thickness d and length l of the beam.

If the applied excitation frequency is equals to the resonance frequency (ω_n) of the system, the PZT transducer converts the maximum instant power the most, and Equation (9) becomes

$$\begin{aligned} P_{c\max} &= \left|P_c(\omega_n)\right| = \frac{k_e m^2 Y_0^2}{2k}\frac{m^2\omega_n^4}{(2\varsigma)^2} = \frac{k_e m^4 Y_0^2 \omega_n^4}{8k\varsigma^2} \\ &= \frac{k_e m^4 Y_0^2 \omega_n^6}{2kb^2} \quad \text{(Appendix B)} \\ &= \frac{3k_e Y_0^2 E^2 \rho}{96}\frac{d^7 w^3}{l^5 b^2} \\ &\propto \left(\frac{3k_e E^2\rho}{96}\right)\left(\frac{d^7 w Y_0^2}{l^7}\right) \end{aligned} \tag{11}$$

It is found from Equation (11) that the maximum converted electric energy is proportional to the electromechanical constant k_e, the beam mass m, the resonance frequency of the mechanical system, and the displacement induced by external force, but is inverse proportional to the equivalent spring constant k and the damping coefficient b.

When the PZT converts the maximum instant power as shown in Equation (11), the induced potential difference V_x reaches the maxima. i.e. $P_{\max} = \frac{1}{2}C_p V_{x\max}^2$. Equation (12) can be used to determine the $V_{x\max}$.

$$V_{x\max}^2 = \frac{k_e m^4 Y_0^2 \omega_n^6}{C_p k b^2} \tag{12}$$

C_p in Equation (12) can be described by

$$C_p = \varepsilon\frac{A}{d} \tag{13}$$

Substituting Equation (13) into Equation (12), we have

$$V_{x\max} = \sqrt{\frac{dk_e m^4 Y_0^2 \omega_n^{\,6}}{\varepsilon A k b^2}}$$
$$= \sqrt{\frac{9\rho E^2 k_e}{144\varepsilon}} \frac{Y_0 w d^4}{b l^3} \quad \text{(Appendix C)} \qquad (14)$$
$$\propto \frac{E}{4}\sqrt{\frac{\rho k_e}{\varepsilon}} \frac{Y_0 d^4}{l^4}$$

From Equation (14), the induced voltage is found to be proportional to the electromechanical constant k_e, the beam mass m, the thickness of PZT film and the displacement induced by external force, but is inverse proportional to the equivalent spring constant k, the damping coefficient b, the area of PZT film, and the dielectric constant ε. For real implementation, the average power deserves more consideration than the instant power. From Equation (14), the average power can be calculated by

$$P_{av} = \frac{T}{2}\int_0^{T/2} \frac{3k_e Y_0^2 E^2 \rho}{96} \frac{l^5 d^7 w^3}{b^2} \cos^2(\omega_n t)\, dt$$
$$= \frac{3k_e Y_0^2 E^3}{3072 \times 4\pi^2} \frac{w^3 d^9}{l^9 b^2} \quad \text{(Appendix D)} \qquad (15)$$
$$\propto \left(\frac{3k_e E^3}{3072 \times 4\pi^2}\right)\left(\frac{w d^9}{l^{11}} Y_0^2\right)$$

By carefully selecting these parameters, it is feasible to design a high efficiency piezoelectric vibration-induced micro power generator.

As an external resistance Z_L is connected to both sides of the PZT film, the induced energy stored in C_p will be consumed by the external load Z_L. The crossing voltage on Z_L can be regard as an additional voltage source applied to the PZT film, such that the vibrating deformation of the PZT is deformed; therefore the induced voltage is reduced. In other word, the conversing efficiency is decreased. Figure 5 shows the enhanced equivalent circuit of the vibration-induced micro power generator.

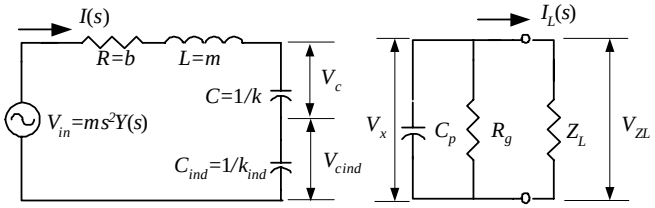

Figure 5. Enhanced equivalent circuit of the vibration-induced micro power generator

In Figure 5, the capacitor C_{ind} is induced by V_{ZL} and can be interpreted as a function of I_L.

$$C_{ind} = f\left(I_L(s)\right) \qquad (16)$$

The equivalent spring constant k_{eq} is

$$k_{eq} = \frac{C + C_{ind}}{C \times C_{ind}} = k + k_{ind} \qquad (17)$$

Equation (17) shows that the load impedance Z_L enlarges the spring constant of the system. The deformation on the PZT and the induced voltage V_x are reduced.

Piezoelectric Vibration-Induced Power Generator

A simplified piezoelectric vibration-induced power generator [4] is shown in Figure 4. When the beam structure vibrates, the piezoelectric film adhered on the beam deforms and induces strain. The induced strain forces the positive and negative charges to be separated on both surfaces of the piezoelectric film and create electrical potential difference. The electrical potential difference can be further converted into usable electricity.

Many piezoelectric materials have been developed. The piezoelectric ceramics possess advantages such as easily to be fabricated and to be able to be manufactured into any shape, have become the major material for piezoelectric devices. Among the piezoelectric ceramics, the PZT has relatively higher degree of electromagnetive coupling and higher Curie temperature. Higher electromagnetive coupling enables high efficiency of energy conversion, while high Curie temperature allows the devices to be implemented in a wider temperature range. In this research, the PZT is selected as the material to build the piezoelectric film.

TRANSDUCER DESIGN, SIMULATION, AND FABRICATION

Transducer Design

To verify the power transformation principle discussed above, two clusters of transducer structures are considered. The schematic layout of the transducer is shown in Figure 6. Dimensions of these two clusters of transducer structures are tabulated in Table 1 and Table 2, respectively. The belonging transducers of the first cluster have same length but different width. The transducers of the second cluster have same width but different length. Physical properties of the copper substrate and the PZT for finite element analysis (FEA) are listed in Table 3.

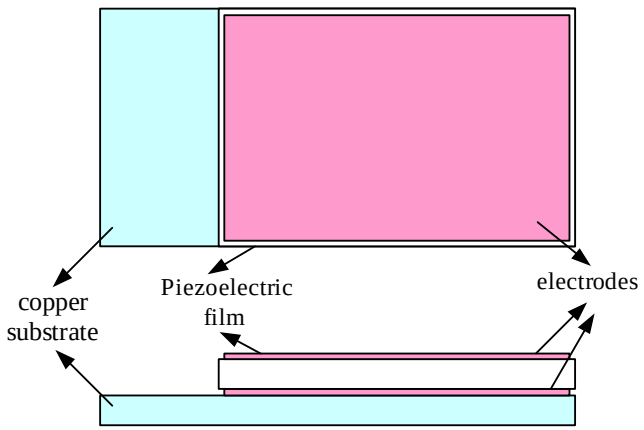

Figure 6. Schematic layout of the transducer

Table 1. Structure of different width

	1A	1B	1C
Copper substrate	*l*=25mm	*l*=25mm	*l*=25mm
	w=10mm	*w*=8mm	*w*=6mm
PZT film	*l*=20mm	*l*=20mm	*l*=20mm
	w=10mm	*w*=8mm	*w*=6mm

Table 2. Structure of different length

	1A	1B	1C
Copper substrate	*l*=26mm	*l*=23mm	*l*=20mm
	w=8mm	*w*=8mm	*w*=8mm
PZT film	*l*=21mm	*l*=18mm	*l*=15mm
	w=8mm	*w*=8mm	*w*=8mm

Table3. Physical properties of the materials

Properties	Copper substrate	PZT
Young's modulus	100 GPa	45 GPa
Density	8,500 kg/m^3	7,600 kg/m^3
Poisson ration	0.3	0.265

Transducer Modal Analysis

According to the theoretical modeling in Section 2, the peak voltage induced by the piezoelectric vibration occurred at the resonance frequency of the transducer structure. To determine the resonance frequency of each structure for further comparisons with the experiments, the ANSYS finite element analysis software is implemented.

Table 4 depicts the first 4 resonance frequencies for each structure. For cluster 1, the first resonance frequencies are almost the same. It coincides with the theoretical results in Equation (10). It is also found that the longer the transducer is, the lower its resonance frequency is. Besides the first mode, all three other modes are much higher. For practical implantations, it is reasonable to consider only the first mode resonance frequency.

Table 4. Resonance frequencies of the transducers

	1A	1B	1C	2A	2B	2C
1st mode	270Hz	269Hz	268Hz	244Hz	323Hz	481Hz
2nd mode	1169Hz	1418Hz	1680Hz	1343Hz	1597Hz	1967Hz
3rd mode	1686Hz	1683Hz	1834Hz	1526Hz	2081Hz	3002Hz
4th mode	3803Hz	4516Hz	4726Hz	4260Hz	5134Hz	6447Hz

Transducer Fabrication

The transducer fabrication procedures are: (1) fabricating the piezoelectric film (2) screen printing the electrodes (3) preparing the substrate (4) adhering and cutting (5) wiring.

(1) Fabricating the piezoelectric film

The ZrO_2, PbO, and TiO_2 maxed powder is calcined into the PZT ceramic powder. The PZT ceramic powder is then pressed and sintered at 900 °C to grow the lead zirconate titanate crystal structure. Following is polarizing the crystal structure with an 4 Kv/mm electric field to form the piezoelectric film. Polarization orientation should be normal to the beam surface.

(2) Screen printing the electrodes

The screen printing technique is adopted to print silver electrodes on top and bottom surfaces of the piezoelectric film.

(3) Preparing the copper substrate

The raw copper plate is roughly polished using emery cloth and followed by a fine polishing using acetone. Surface cleaning is then processed by ultrasonic.

(4) Adhering and cutting

The PZT film is adhered on the top surface of the copper substrate with epoxy resin. A micro CNC machining center is adopted to machine it into desired shapes.

(5) Wiring

Solder the conducting wires to the electrodes to complete the fabrication processes.

POWER GENERATING TESTING AND ELECTRICITY CHARGING

Power Generating Testing

The apparatus for power generating test is illustrated in Figure 7 and tabulated in Table 5. The signal generator is to provide sinusoidal signals with different frequencies. The ambient vibrations are simulated by the electromechanical shaker. The laser interferometer is used to ensure that the amplitudes of different sinusoidal signals from the electromechanical shaker are the same. During our experiments, the amplitude is set to be 20 μm. The induced voltages from the generator are measured through the oscilloscope.

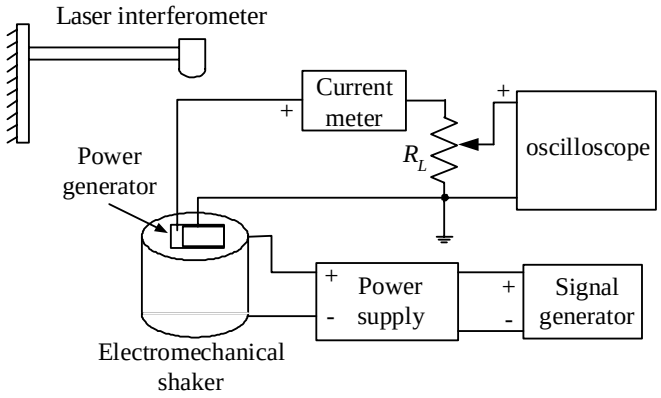

Figure 7. Power generating testing apparatus

Table 5. Power generating testing equipments

Signal generator	Power supply	Shaker	Current meter	Oscill.	Laser interfere
HP 8904A	B&K 2706	B&K 4809	YFE YF-3502	HITACH I V-212	SIOS

Figure 8 and Figure 9 illustrate the no load responses of the two clusters, respectively. Table 6 shows the peak voltages of each structure and their relevant frequencies. The responses indicate that the maximum output voltages are generated in accordance with the first mode resonance frequencies calculated by the ANSYS analysis. It is also found from the experimental results that the induced voltage is irrelevant to the width of the structure but is inverse proportion to the length of the structure. These results are coincidence with the theoretical analysis in Section 2.

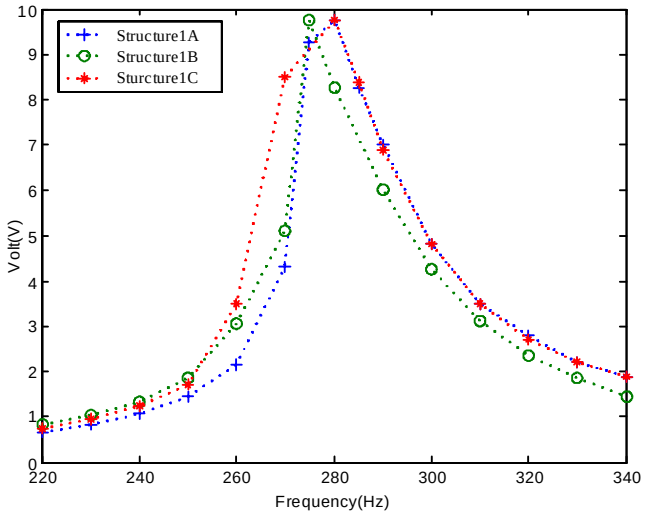

Figure 8. No load responses of cluster 1

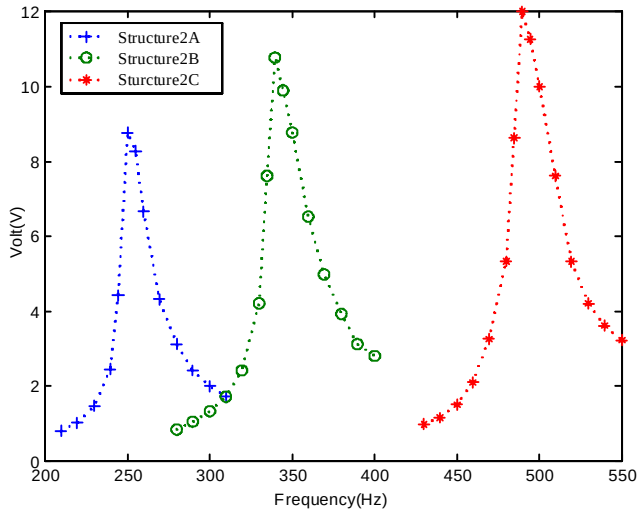

Figure 9. No load responses of cluster 2

Table 6. Peak voltages and relevant frequencies

	1A	1B	1C	2A	2B	2C
ω_n	280Hz	275Hz	280Hz	250Hz	340Hz	490Hz
V_{peak}	9.75 V	9.75 V	9.75 V	8.75 V	10.75 V	12.0 V

Figure 10 and Figure 11 show the output powers measured when an external resistance load is connected between the two electrodes and the input frequency is set at the first mode resonance. Table 7 tabulated the peak output powers and their relevant resistance, cross voltages, and through currents. The output power measurements indicate that the larger the external resistor is, the larger the measured voltage is and the smaller the through current is. It is also found the larger the external resistor is, the larger the amplitude of the piezoelectric beam is.

From Table 7, we can observe that the output powers of the cluster 1 structures are very close. The maximum output power of structure 1A is detected to be a little bit higher then the others two. It is inferred that the internal parallel resistance R_g of structure 1A is lager due to its relatively smaller width; therefore, the transformable power is reduced. For the results of cluster 2, the output power is sharply inverse proportion to the structure length. The output power measurements can verify the theoretical results in Section 2.

Table 7. Peak output power and relevant resistance, voltage, and current

	1A	1B	1C	2A	2B	2C
$Power_{peak}$	1284 μW	1109 μW	1067 μW	833 μW	1753 μW	2870 μW
Resister	15 kΩ	17 kΩ	22 kΩ	20 kΩ	13 kΩ	10 kΩ
Voltage	5.2 V	5.1 V	5.8 V	4.9 V	5.6 V	6.35 V
Current	247 μA	211 μA	184 μA	170 μA	313 μA	452 μA

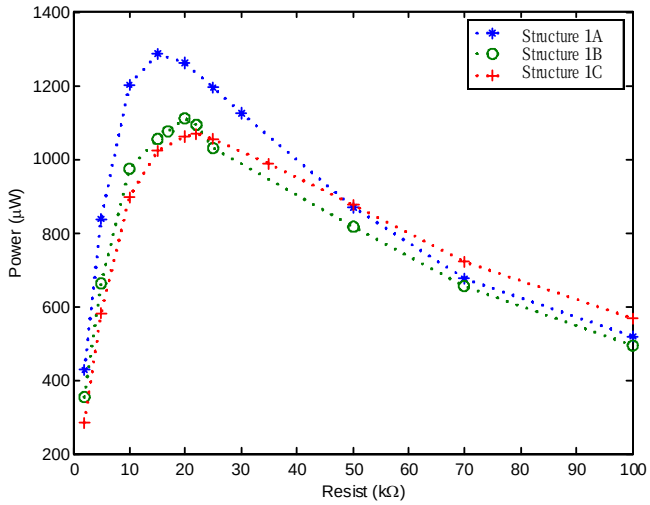

Figure 10. Output power measurement of cluster 1

Electricity Charging

The charging circuit for the vibration induced power generator is shown in Figure 12. The bridge circuit is to rectify the vibration-induced AC current to the DC form. A 10,000 μF capacitor that is constituted by 100 parallel connected 100 μF capacitors. Figure 13 shows the charging results of cluster 1 structures. It takes 7 minutes to charge the capacitors array to a 7 V level. The total amount of electricity and energy stored are 0.7 Coulomb and 0.245 J, respectively.

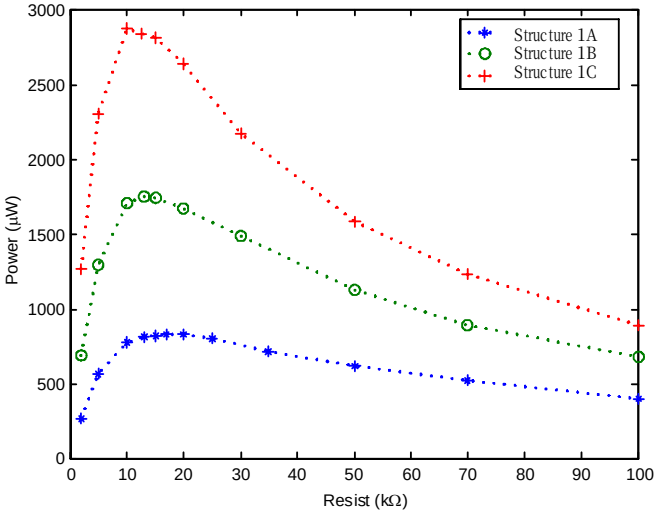

Figure 11. Output power measurement of cluster 2

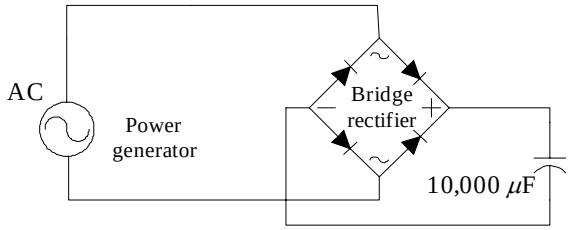

Figure 12. Charging circuit

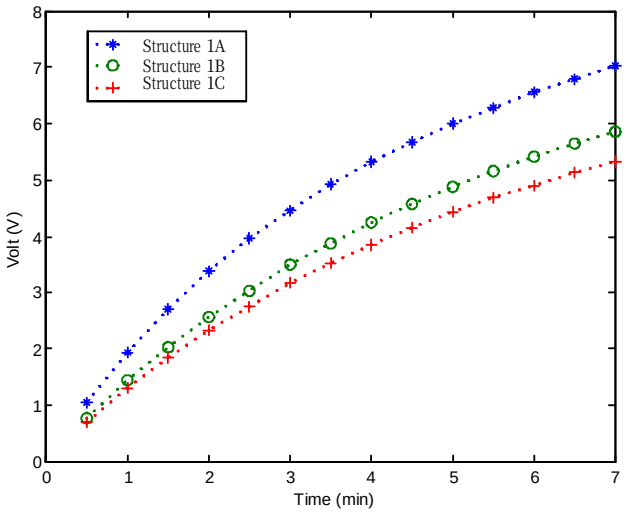

Figure 13. Charging results

CONCLUSION

In this article, theoretical and experimental study of a piezoelectric vibration-induced micro power generator that can convert mechanical vibration energy into electrical energy is presented.

A complete mechanical-electrical energy conversion model regarding the piezoelectric transducer is discussed first. The desired shape of the transducer with its first mode resonance frequency in accordance with the ambient vibration source can be designed by the finite element analysis software, ANSYS. To verify the theoretical analysis, two clusters of transducer structures are fabricated. The oscillation source of the micro generator is a copper plate. A piezoelectric film with 1 μm thickness of silver electrode layer being screen printed on both the top and bottom surfaces is attached on the copper substrate. The piezoelectric film that plays the role as the transducer for energy conversion is made of the piezoelectric lead zirconate titanate (PZT). The PZT film that has better energy conversion efficiency among the piezoelectric materials is formed by the sintering method and cut into the desired shape by a CNC micro machining center.

Conducting wires and load resistor are soldered on the electrodes to output and measure the vibration induced electrical power. An electromechanical shaker with tunable frequency is employed to verify the performance of the proposed micro inertia generator. Experimental results demonstrate that the maximum output voltages are occurred at the first mode resonance frequencies of the structure. It is also found from the experimental results that the induced voltage is irrelevant to the width of the structure but is inverse proportion to the length of the structure. The output power measurements indicate that the larger the external resistor is, the larger the measured voltage is and the smaller the through current is. It takes 7 minutes to charge a 10,000 μF capacitors array to a 7 V level. The total amount of electricity and energy stored in the capacitors are 0.7 Coulomb and 0.245 J, respectively. The experimental results are coincidence with the theoretical analysis.

ACKNOWLEDGMENTS

The authors would like to thank the National Science Council of Taiwan for financial support under the grant NSC-91-2212-E-005-012. The authors would also like to thank the Mechanical Industry Research Laboratories of the Industrial Technology Research Institute, Taiwan, for financial support to complete this research.

APPENDIX

Appendix A: resonance frequency

$$\omega_n = \sqrt{\frac{k}{M}} \tag{A1}$$

Where k is the spring constant and M is the mass of the beam.

$$k = \frac{W}{\delta} = \frac{3EI}{l^3} \tag{A2}$$

Where E is Young modulus, l is the length of the beam, and I is moment of inertia.

$$I = \frac{wd^3}{12} \tag{A3}$$

where w and d are the width and thickness of the beam, respectively.

From Equations (A1) , (A2) and (A3), it is found that

$$\omega_n = \sqrt{\frac{3EI}{Ml^3}} = \sqrt{\frac{3Ewd^3}{12(\rho lwd)l^3}} = \frac{d}{2l^2}\sqrt{\frac{E}{\rho}} \tag{A4}$$

where ρ is the mass density of the beam. ω_n is only depending on d and l.

Appendix B : Instant Power

From Equation (11),

$$P_{c\max} = \frac{k_e Y_0^2}{2}\frac{m^4\omega_n{}^6}{kb^2} = \frac{k_e Y_0^2}{2}\frac{(\rho lwd)^4\left(\frac{d}{2l^2}\right)^6\left(\frac{E}{\rho}\right)^3}{\frac{3EI}{l^3}b^2}$$

$$= \frac{k_e Y_0^2}{2}\frac{12(\rho lwd)^4 l^3 d^6 E^3}{192 l^{12}\rho^3 E w d^3 b^2} \qquad \text{(A5)}$$

$$= \frac{3k_e Y_0^2 E^2 \rho}{96}\frac{d^7 w^3}{l^5 b^2}$$

$$\propto \left(\frac{3k_e E^2\rho}{96}\right)\left(\frac{d^7 w Y_0^2}{l^7}\right)$$

Appendix C: Induced Voltage

From Equation (14), (A1), (A2), (A3), and (A4), we have

$$V^2{}_{x\max} = \left(\frac{9\rho E^2 k_e}{144\varepsilon}\right)\frac{Y_0{}^2 w^2 d^8}{b^2 l^6} \qquad \text{(A6)}$$

Since the damping coefficient *b* is proportional to the area of the beam, it can be inferred from Equation (A5) that

$$V_{x\max} \propto \frac{E}{4}\sqrt{\frac{\rho k_e}{\varepsilon}}\frac{Y_0 d^4}{l^4} \qquad \text{(A7)}$$

We conclude that the induced voltage is proportional to Y_0 and *d*, inverse proportional to *l*.

Appendix D: Average Power P_{av}

$$P_{av} = \frac{T}{2}\int_0^{T/2}\frac{3k_e Y_0^2 E^2\rho}{96}\frac{d^7 w^3}{l^5 b^2}\cos^2(\omega_n t)\,dt$$

$$= \frac{3k_e Y_0^2 E^2\rho}{96}\frac{d^7 w^3}{l^5 b^2}\frac{T}{2}\int_0^{\frac{T}{2}}\cos^2\left(\frac{2\pi}{T}t\right)dt \qquad \text{(A8)}$$

$$= \frac{3k_e Y_0^2 E^2\rho}{96}\frac{d^7 w^3}{l^5 b^2}\frac{T^2}{8}$$

$$= \frac{3k_e Y_0^2 E^2\rho}{768}\frac{d^7 w^3}{l^5}\frac{T^2}{b^2}$$

$$= \frac{3k_e Y_0^2 E^2\rho}{768}\frac{d^7 w^3}{l^5}\frac{\omega_n{}^2}{(2\pi)^2 b^2}$$

$$= \frac{3k_e Y_0^2 E^2\rho}{768}\frac{d^7 w^3}{l^5}\left(\frac{d}{2l^2}\sqrt{\frac{E}{\rho}}\right)^2\frac{1}{4\pi^2 b^2}$$

$$= \frac{3k_e Y_0^2 E^2\rho}{768\pi^2}\frac{d^7 w^3}{l^5}\frac{d^2 E}{4l^4\rho b^2}$$

$$= \frac{3k_e Y_0^2 E^3}{3072\times 4\pi^2}\frac{w^3 d^9}{l^9 b^2}$$

$$\propto \left(\frac{3k_e E^3}{3072\times 4\pi^2}\right)\left(\frac{d^9 w}{l^{11}}Y_0^2\right)$$

REFERENCES

[1] Koeneman, P. B., Busch-Vishiac, I. J., and Wood, K. L., 1997, "Feasibility of micro power supplies for MEMS", *Journal of Microelectromechanical Systems*, 6(4), pp. 355- 362.

[2] Rowe, D. M., Morgan, D. V., and Kiely, J. H., 1991, "Low cost miniature thermoelectric generator", *Electronic Letter*, 27, pp. 2332-2334.

[3] Glynne-Jones, P., Beeby, S. P., and White, N. M., 2001, " Toward piezoelectric vibration-powered microgenerator", *IEE Proc.-Sci. Meas. Technol.*, 148(2), pp. 68-72.

[4] Kang, J. Y., Kim, H. J., Kim, J. S., Kim, T. S., 2002, "Optimal design of piezoelectric cantilever for a micro power generator with microbubble", *The 2nd Annual International IEEE-EMBS Special Topic Conference on Microtechnologies in Medicine & Biology*, pp. 424-427.

[5] Kasyap, A., Kim, J. S., Ngo, K., Kurdial, A., Nishida, T., Sheplak, M., and Cattafesta, L., 2002, "Energy Reclamation from a Vibrating Piezoceramic Composite Beam", *Proceeding of the 9th International Congress on Sound and Vibration*, pp. 36-43.

[6] Williams, C. B. and Yates, R. B., 1995, "Analysis of a micro-electric generator for Microsystems", *Proceeding of the 8th International Conference on Solid-State Sensors and Actuators*, 1, pp. 369-372.

[7] Williams, C. B., Woods, R. C. and Yates, R. B., 1996, "Feasibility study of a vibration powered micro-electric generator", *Compact Power Sources* (*Digest No. 96/107*), *IEE Colloquium*, pp. 7/1-7/3.

[8] Amirtharajah, R. and Chandrakasan, A. P., 1998, "Self-powered signal processing using vibration-based power generation," *IEEE Journal of Solid-State Circuits*, 33(5), pp. 687-695.

[9] Williams, C. B., Shearwood, C., Harradine, M. A., Mellor, P. H., Birch, T. S., and Yates, R. B., 2001, "Development of an electromagnetic micro-generator," *IEE Porc.-Circuits Devices System*, 148(6), pp. 337-342.

[10] Li, W. J., Wen, Z., Wong, P. K., Chan, G. M. H., and Leong, P. H. W., 2000, "A microchined vibration-induced power generator for low power sensors of robotic systems", *Proceeding of the 8th International Symposium on Robotics with Application*, pp. 16-21.

[11] Li, W. J., Ho, T. C. H., Chan, G. M. H., Leong, P. H. W., and Wong, H. Y., 2000, "Infrared signal transmission by a laser-micromachined vibration-induced power generator," *Proceeding of the 43th IEEE Midwest Symposium on Circuits and Systems*, pp. 236-239.